

Transit cosmological models in Myrzakulov $F(R, T)$ gravity theory

Dinesh Chandra Maurya¹, Ratbay Myrzakulov²

¹ Centre for Cosmology, Astrophysics and Space Science, GLA University, Mathura-281 406, Uttar Pradesh, India.

² Eurasian International Centre for Theoretical Physics and Department of General & Theoretical Physics, Eurasian National University, Astana 010008, Kazakhstan.

¹Email:dcmaurya563@gmail.com

²Email:rmyrzakulov@gmail.com

Abstract

In the present paper, we investigate some exact cosmological models in Myrzakulov $F(R, T)$ gravity theory. We have considered the arbitrary function $F(R, T) = R + \lambda T$ where λ is an arbitrary constant, R, T are respectively, the Ricci-scalar curvature and the torsion. We have solved the field equations in a flat FLRW spacetime manifold for Hubble parameter and using the MCMC analysis, we have estimated the best fit values of model parameters with $1 - \sigma, 2 - \sigma, 3 - \sigma$ regions, for two observational datasets like $H(z)$ and Pantheon SNe Ia datasets. Using these best fit values of model parameters, we have done the result analysis and discussion of the model. We have found a transit phase decelerating-accelerating universe model with transition redshifts $z_t = 0.532, 0.435$. The effective dark energy equation of state varies as $-1 \leq \omega_{de} \leq -0.993$ and the present age of the universe is found as $t_0 = 13.92, 13.65$ Gyrs, respectively for two datasets.

Keywords: Myrzakulov $F(R, T)$ gravity; Exact solutions; FLRW Universe; Transit Universe; Observational Constraints.

PACS number: 98.80-k, 98.80.Jk, 04.50.Kd

Contents

1	Introduction	2
2	Myrzakulov $F(R, T)$ gravity and field equations	3
3	Cosmological solutions for $F(R, T) = R + \lambda T$	4
4	Observational Constraints	5
4.1	Hubble Function	5
4.2	Apparent Magnitude $m(z)$	8
5	Result Analysis and Discussion	9
6	Age of the Universe	12
7	Conclusions	13

1 Introduction

The universe underwent two episodes of accelerated expansion at early and late times of the cosmological evolution, according to the conventional paradigm of cosmology, which is based on a growing amount of observable data. Although the cosmological constant might be the best explanation for late time acceleration, the possibility that the acceleration is dynamic in nature and the presence of some potential tensions may call for a revision of our understanding—something that is unquestionably necessary for early time acceleration. There are primarily two paths one could take in order to accomplish this. The first is to build extended gravitational theories that, although having general relativity as a specific limit, can generally offer more degrees of freedom to adequately describe the evolution of the universe [1, 2]. The second approach is to modify the conventional particle physics model and take general relativity into account. This involves assuming that the universe contains additional matter in the form of dark energy [3, 4] and/or inflation fields [5]. Keep in mind that the first approach has the extra theoretical benefit of may be leading to an improved.

One can begin building gravitational modifications from the Einstein-Hilbert action, that is, from the curvature description of gravity, and extend it appropriately, as in the cases of Lovelock gravity [11, 12], $F(R)$ gravity [8], and $F(G)$ gravity [9, 10]. He may also examine torsional modified gravities, such as $F(T)$ gravity [15, 16, 17], $F(T, T_G)$ gravity [18], etc., starting with the analogous, teleparallel formulation of gravity in terms of torsion [13, 14]. Additionally, nonmetricity could be used to create gravitational alterations [19]. Furthermore, altering the fundamental geometry itself might give rise to an intriguing class of modified gravity; this could include, for example, Finsler or Finsler-like geometries [20]-[23]. The non-linear connection's potential to introduce additional degrees of freedom and make the gravitational modification phenomenologically interesting is one of the framework's intriguing features [24, 25]. This feature was also obtained through the use of a different theoretical framework for metric-affine theories [27, 28, 29].

In [30], R. Myrzakulov found an intriguing gravitational modification called the $F(R, T)$ gravity. Both curvature and torsion are dynamical fields associated with gravity in this theory because one makes use of a particular but non-special connection. Because of this, the theory has additional degrees of freedom originating from both the non-special connection and the arbitrary function in the Lagrangian. The theory belongs to the class of Riemann-Cartan theories, which are part of the broader category of metric theories with affine connections [31, 32]. A few of the theory's applications were examined in [30] and [33]–[36]. Specifically, [30] addressed certain theoretical concerns; [33] examined energy conditions; [34] examined theoretical relationships with various scenarios; [35] examined Noether symmetries; and [36] examined neutron star theory. Recently, in [37] have analyzed the resultant cosmology of such a framework and to compute the evolution of observable quantities like the effective dark energy equation-of-state parameter and density parameters. By expressing the theory as a deformation from both general relativity and its teleparallel counterpart, they have examined the cosmological behavior with an emphasis on the connection's effect by employing the mini-super-space approach. The observational constraints on Myrzakulov $F(R, T)$ -gravity have been investigated in [38]. Various Metric-Affine Myrzakulov Gravity Theories and its applications are discussed in [39]-[45].

Motivated by the above discussions, in this paper, we investigate a spatially flat, isotropic and homogeneous spacetime universe in Myrzakulov $F(R, T)$ Gravity. The paper is organized as follows. In Section 2, we give a brief review of the Myrzakulov $F(R, T)$ gravity theory. The cosmological solution for the particular linear case $F(R, T) = R + \lambda T$ are given in Section 3. Observational constraints for the model are studied in Section 4. The result analysis and discussions are presented in Section 5. The age of the universe is considered in Section 6. The last Sec. 7 is devoted to conclusions.

2 Myrzakulov $F(R, T)$ gravity and field equations

To explore the cosmological properties of the universe in Myrzakulov $F(R, T)$ gravity, we consider the flat FRW space-time described by the metric

$$ds^2 = -dt^2 + a^2(t)(dx^2 + dy^2 + dz^2), \quad (1)$$

where $a = a(t)$ is the scale factor. The orthonormal tetrad components $e_i(x^\mu)$ are related to the metric through

$$g_{\mu\nu} = \eta_{ij} e_\mu^i e_\nu^j, \quad (2)$$

where the Latin indices i, j run over 0...3 for the tangent space of the manifold, while the Greek letters μ, ν are the coordinate indices on the manifold, also running over 0...3.

We consider the action for Myrzakulov $F(R, T)$ gravity [30, 37] as

$$S = \int e[F(R, T) + L_m]dx^4, \quad (3)$$

where $e = \sqrt{-g}$ with g as the determinant of metric tensor $g_{\mu\nu}$, $R = R^{(LC)} + u$ and $T = T^{(W)} + v$ with $R^{(LC)}$ is the Ricci scalar corresponding to Levi-Civita connection and $T^{(W)}$ is the torsion scalar corresponding to Weitzenböck connection. And u is a scalar quantity depending on the tetrad, its first and second derivatives, and the connection and its first derivative, and v is a scalar quantity depending on the tetrad, its first derivative and the connection. Hence, u and v quantify the information on the specific imposed connection [37].

In this paper, we restrict ourselves to the case $u = u(a, \dot{a})$ and $v = v(a, \dot{a})$. The scale factor $a(t)$, the curvature scalar R and the torsion scalar T are taken as independent dynamical variables. Then after some algebra the action (3) becomes [46],

$$S = \int L dt, \quad (4)$$

where the point-like Lagrangian is given by

$$L = a^3(F - TF_T - RF_R + vF_T + uF_R) - 6(F_R + F_T)a\dot{a}^2 - 6(F_{RR}\dot{R} + F_{RT}\dot{T})a^2\dot{a} - a^3L_m. \quad (5)$$

The corresponding field equations of Myrzakulov $F(R, T)$ gravity are obtained in [46, 47], as

$$3H\dot{R}F_{RR} - 3(\dot{H} + H^2)F_R + 3H\dot{T}F_{RT} + 6H^2F_T + \frac{1}{2}F - \frac{1}{2}\dot{a}u_{\dot{a}}F_R - \frac{1}{2}\dot{a}v_{\dot{a}}F_T = \rho, \quad (6)$$

$$\begin{aligned} & \dot{R}^2 F_{RRR} + (\ddot{R} + 2\dot{R}H)F_{RR} + (3H^2 + 2\dot{H} - \frac{1}{2}R)(F_R + F_T) + 2\dot{T}HF_{TT} + 2\dot{R}\dot{T}F_{RRT} + \dot{T}^2F_{RTT} \\ & + (2\dot{R}H + 2\dot{T}H + \ddot{T})F_{RT} + \frac{1}{2}F - \frac{1}{6}au_{\dot{a}}\dot{R}F_{RR} - (\frac{1}{2}\dot{a}u_{\dot{a}} + \frac{1}{6}a\dot{u}_{\dot{a}} - \frac{1}{2}u - \frac{1}{6}au_a)F_R - \frac{1}{6}av_{\dot{a}}\dot{T}F_{TT} \\ & - (\frac{1}{2}\dot{a}v_{\dot{a}} + \frac{1}{6}a\dot{v}_{\dot{a}} - \frac{1}{2}v - \frac{1}{6}av_a)F_T - \frac{1}{6}a(v_{\dot{a}}\dot{R} + u_{\dot{a}}\dot{T})F_{RT} = -p. \end{aligned} \quad (7)$$

The energy conservation equation is obtained as

$$\dot{\rho} + 3H(\rho + p) = 0. \quad (8)$$

3 Cosmological solutions for $F(R, T) = R + \lambda T$

In this investigation, we take the arbitrary function $F(R, T)$ in linear form in R and T as given by

$$F(R, T) = R + \lambda T, \quad (9)$$

where λ is an arbitrary constant, $R = u + 6(\dot{H} + 2H^2)$ and $T = v - 6H^2$. Using Eq. (9) in Eqs. (6) & (7), we obtain the field equations in the form

$$3(1 + \lambda)H^2 + 0.5[(u - \dot{a}u_{\dot{a}}) + \lambda(v - \dot{a}v_{\dot{a}})] = \rho, \quad (10)$$

and

$$(1 + \lambda)(2\dot{H} + 3H^2) + 0.5[u - \dot{a}u_{\dot{a}} - \frac{1}{3}a\dot{u}_{\dot{a}} + \frac{1}{3}au_{\dot{a}}] + 0.5\lambda[v - \dot{a}v_{\dot{a}} - \frac{1}{3}a\dot{v}_{\dot{a}} + \frac{1}{3}av_{\dot{a}}] = -p. \quad (11)$$

Now, we consider the scalars u and v in the form of [44]

$$u = c_1 \frac{\dot{a}}{a} \ln \dot{a}, \quad v = s(a)\dot{a}, \quad (12)$$

where c_1 is an arbitrary constant and $s(a)$ is an arbitrary function of scale factor a .

Using Eq. (12) in Eqs. (10) & (11), we get the following form of the field equations (10) & (11):

$$3(1 + \lambda)H^2 - \frac{1}{2}c_1H = \rho, \quad (13)$$

$$(1 + \lambda)(2\dot{H} + 3H^2) - \frac{1}{2}c_1H - \frac{1}{6}c_1\frac{\dot{H}}{H} = -p. \quad (14)$$

For $\lambda = 0, c_1 = 0$, the field equations, (13) & (14) will reduced into original Einstein's field equations in general relativity (GR). One can obtain the Friedmann like equations as

$$3H^2 = \rho + \rho_{MG}, \quad (15)$$

$$2\dot{H} + 3H^2 = -p - p_{MG}, \quad (16)$$

where ρ_{MG}, p_{MG} are the geometrical corrections in energy density and pressure, respectively given by

$$\rho_{MG} = \frac{1}{2}c_1H - 3\lambda H^2, \quad p_{MG} = - \left[\frac{1}{2}c_1H + \frac{1}{6}c_1\frac{\dot{H}}{H} - \lambda(2\dot{H} + 3H^2) \right]. \quad (17)$$

These, geometrical corrections, respectively, in energy density and pressure ρ_{MG}, p_{MG} , called as effective dark energy sector in Myrzakulov gravity. We can show that effective dark energy sector is conserved, namely $\dot{\rho}_{MG} + 3H(\rho_{MG} + p_{MG}) = 0$, and it can be easily deduced from matter energy conservation equation $\dot{\rho} + 3H(\rho + p) = 0$. We define the matter equation of state as $p = \omega\rho$ with $\omega = \text{constant}$ and using Eqs. (13) & (14), we get

$$\frac{12(1 + \lambda)H - c_1}{6H}\dot{H} + \frac{6(1 + \lambda)H^2 - c_1H}{2}(1 + \omega) = 0, \quad (18)$$

or

$$\frac{12(1 + \lambda)H - c_1}{6(1 + \lambda)H^2 - c_1H}dH + 3(1 + \omega)\frac{da}{a} = 0. \quad (19)$$

After integration Eq. (19), we get

$$6(1 + \lambda)H^2 - c_1H - c_2 \left(\frac{a_0}{a} \right)^{3(1+\omega)} = 0, \quad (20)$$

where c_2 is an integrating constant.

Solving Eq. (20) for Hubble parameter H , we obtain

$$H(a) = \frac{c_1}{12(1+\lambda)} + \frac{1}{12} \sqrt{\left(\frac{c_1}{1+\lambda}\right)^2 + \left(\frac{24c_2}{1+\lambda}\right) \left(\frac{a_0}{a}\right)^{3(1+\omega)}}, \quad \lambda \neq -1. \quad (21)$$

For $c_1 = 0$, we get Hubble parameter as $H(a) = \frac{\sqrt{6c_2}}{6\sqrt{1+\lambda}} \left(\frac{a_0}{a}\right)^{3(1+\omega)/2}$ which gives a power-law expansion cosmology with a constant deceleration parameter (DP). If we take $c_2 = 0$, then we find $H = \text{constant}$ which gives exponential-law expansion cosmology with constant DP.

Using the relation $\frac{a_0}{a} = 1 + z$ [3], we get

$$H(z) = \frac{c_1}{12(1+\lambda)} + \frac{1}{12} \sqrt{\left(\frac{c_1}{1+\lambda}\right)^2 + \left(\frac{24c_2}{1+\lambda}\right) (1+z)^{3(1+\omega)}}, \quad \lambda \neq -1. \quad (22)$$

The deceleration parameter is derived from $q = -1 + (1+z)\frac{H'}{H}$ as

$$q(z) = -1 + \frac{36(1+\omega)c_2(1+z)^{3(1+\omega)}}{\frac{c_1^2}{1+\lambda} + 24c_2(1+z)^{3(1+\omega)} + c_1 \sqrt{\left(\frac{c_1}{1+\lambda}\right)^2 + \frac{24c_2}{1+\lambda}(1+z)^{3(1+\omega)}}}, \quad \lambda \neq -1. \quad (23)$$

4 Observational Constraints

For our model and dataset combination, we use the freely available emcee program, available at [48], to conduct an MCMC (Monte Carlo Markov Chain) analysis so that we may compare the model with observational datasets. Through parameter value variation across a variety of cautious priors and analysis of the parameter space posteriors, the MCMC sampler constrains the model and cosmological parameters. We then obtain the one-dimensional and two-dimensional distributions for each parameter: the one-dimensional distribution represents the posterior distribution of the parameter, whilst the two-dimensional distribution shows the covariance between two different values.

4.1 Hubble Function

To ensure the model's validity and feasibility, a model that aligns with observational datasets must be obtained. As a result, in order to obtain this condition, we first investigated 32 observed Hubble datasets $H(z)$ across redshift z , with $H(z)$ [49]-[56] having errors (see Table 1). We used the following χ^2 -test formula while fitting data:

$$\chi^2(c_1, c_2, \lambda, \omega) = \sum_{i=1}^{i=N} \frac{[(H_{ob})_i - (H_{th})_i]^2}{\sigma_i^2}$$

Where N denotes the total amount of data, H_{ob} , H_{th} , respectively, the observed and hypothesized datasets of $H(z)$ and standard deviations are displayed by σ_i .

“S.No.	z	$H(z)$	σ_H	Reference
1	0.07	69.0	19.6	[49]
2	0.09	69.0	12.0	[50]
3	0.12	68.6	26.2	[49]
4	0.17	83.0	8.0	[50]
5	0.179	75.0	4.0	[51]
6	0.199	75.0	5.0	[51]
7	0.2	72.9	29.6	[49]
8	0.27	77.0	14.0	[50]
9	0.28	88.8	36.6	[49]
10	0.352	83.0	14.0	[51]
11	0.3802	83.0	13.5	[52]
12	0.4	95.0	17.0	[50]
13	0.4004	77.0	10.2	[52]
14	0.4247	87.1	11.2	[52]
15	0.4497	92.8	12.9	[52]
16	0.47	89.0	50.0	[53]
17	0.4783	80.9	9.0	[52]
18	0.48	97.0	62.0	[54]
19	0.593	104.0	13.0	[51]
20	0.68	92.0	8.0	[51]
21	0.75	98.8	33.6	[55]
22	0.781	105.0	12.0	[51]
23	0.875	125.0	17.0	[51]
24	0.88	90.0	40.0	[54]
25	0.9	117.0	23.0	[50]
26	1.037	154.0	20.0	[51]
27	1.3	168.0	17.0	[50]
28	1.363	160.0	33.6	[56]
29	1.43	177.0	18.0	[50]
30	1.53	140.0	14.0	[50]
31	1.75	202.0	40.0	[50]
32	1.965	186.0	50.4	[56]”

Table 1: Observed values of $H(z)$.

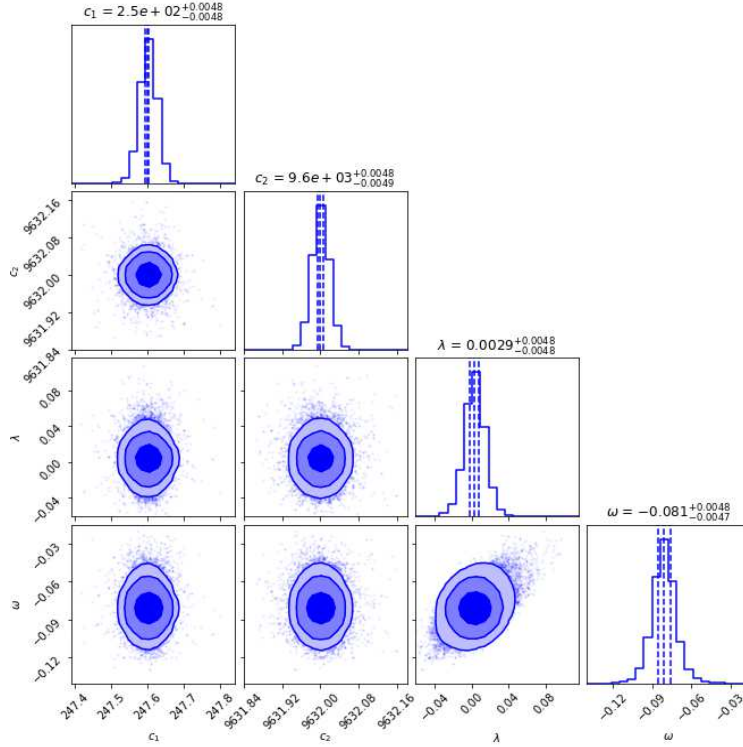


Figure 1: The contour plots of $c_1, c_2, \lambda, \omega$ at $1 - \sigma, 2 - \sigma$ and $3 - \sigma$ confidence level in MCMC analysis of $H(z)$ datasets.

Parameter	Prior	Value
c_1	(10, 1000)	$247.6^{+0.0048}_{-0.0048}$
c_2	(1000, 10000)	$9632^{+0.0048}_{-0.0049}$
λ	(-1, 1)	$0.0029^{+0.0048}_{-0.0048}$
ω	(-1, 1)	$-0.081^{+0.0048}_{-0.0047}$
χ^2	-	17.6422

Table 2: The MCMC Results in $H(z)$ datasets analysis.

The contour plots for parameters c_1, c_2, λ , and ω at 68%, 95%, and 99% confidence levels, respectively, are shown in Figure 1. As indicated in Table 2, we have selected a broad range of priors for our study in order to estimate the cosmological parameters, which have the highest likelihood of existing for the theoretical values of these parameters for the best-fit model. We have estimated best fit values of $c_1 = 247.6^{+0.0048}_{-0.0048}$, $c_2 = 9632^{+0.0048}_{-0.0049}$, $\lambda = 0.0029^{+0.0048}_{-0.0048}$ and $\omega = -0.081^{+0.0048}_{-0.0047}$ at $1 - \sigma, 2 - \sigma$ and $3 - \sigma$ errors using the priors (10, 1000), (1000, 10000), (-1, 1) and (-1, 1), respectively. We have estimated the Hubble constant as $H_0 = 65.5622^{+0.3148}_{-0.3148} \text{ Kms}^{-1} \text{ Mpc}^{-1}$ for the best fit model. Recently, Cao and Ratra [57] have obtained the value of Hubble constant $H_0 = 69.8 \pm 1.3 \text{ Kms}^{-1} \text{ Mpc}^{-1}$ while in [58] they estimated this value as $H_0 = 69.7 \pm 1.2 \text{ Kms}^{-1} \text{ Mpc}^{-1}$. Recently, Alberto Domínguez et al. [59] have obtained this parameter in their likelihood analysis of wide observational datasets as $H_0 = 66.6 \pm 1.6 \text{ Kms}^{-1} \text{ Mpc}^{-1}$ and [60, 61] have obtained as $H_0 = 65.8 \pm 3.4 \text{ Kms}^{-1} \text{ Mpc}^{-1}$. Freedman et al. [62] have estimated the present value of Hubble constant $H_0 = 69.6 \pm 0.8 \text{ Kms}^{-1} \text{ Mpc}^{-1}$, Birrer et al. [63] have measured $H_0 = 67.4^{+4.1}_{-3.2} \text{ Kms}^{-1} \text{ Mpc}^{-1}$, Boruah et al. [64] have measured $H_0 = 69^{+2.9}_{-2.8} \text{ Kms}^{-1} \text{ Mpc}^{-1}$ and most recently, Freedman [65] has estimated $H_0 = 69.8 \pm 0.6 \text{ Kms}^{-1} \text{ Mpc}^{-1}$ and Qin Wu et al. [66] have measured $H_0 = 68.81^{+4.99}_{-4.33} \text{ Kms}^{-1} \text{ Mpc}^{-1}$. Recently, in 2018 [67], the Planck Collaboration estimated that the Hubble constant is currently $H_0 = 67.4 \pm 0.5 \text{ km/s/Mpc}$, while Riess et al. [68] obtained $H_0 = 73.2 \pm 1.3 \text{ km/s/Mpc}$ in 2021. In comparison of the above results, the result obtained in our model for H_0 is compatible with observational

datasets.

4.2 Apparent Magnitude $m(z)$

The relationship between luminosity distance and redshift is one of the main observational techniques used to track the universe's evolution. The expansion of the cosmos and the redshift of the light from distant brilliant objects are taken into consideration when calculating the luminosity distance (D_L) in terms of the cosmic redshift (z). It is provided as

$$D_L = a_0 r(1 + z), \quad (24)$$

where the radial coordinate of the source r , is established by

$$r = \int_0^r dr = \int_0^t \frac{cdt}{a(t)} = \frac{1}{a_0} \int_0^z \frac{cdz}{H(z)}, \quad (25)$$

where we have used $dt = dz/\dot{z}$, $\dot{z} = -H(1 + z)$.

As a result, the luminosity distance is calculated as follows:

$$D_L = c(1 + z) \int_0^z \frac{dz}{H(z)}. \quad (26)$$

Hence, the apparent magnitude $m(z)$ of a supernova is defined as:

$$m(z) = 16.08 + 5 \log_{10} \left[\frac{(1 + z)H_0}{0.026} \int_0^z \frac{dz}{H(z)} \right]. \quad (27)$$

We use the most recent collection of 1048 datasets of the Pantheon SNe Ia samples in the ($0.01 \leq z \leq 1.7$) range [69] in our MCMC analysis. We have used the following χ^2 formula to constrain different model parameters:

$$\chi^2(c_1, c_2, \lambda, \omega, H_0) = \sum_{i=1}^{i=N} \frac{[(m_{ob})_i - (m_{th})_i]^2}{\sigma_i^2}.$$

The entire amount of data is denoted by N , the observed and theoretical datasets of $m(z)$ are represented by m_{ob} and m_{th} , respectively, and standard deviations are denoted by σ_i .

Parameter	Prior	Value
c_1	(10, 1000)	$244_{-0.0039}^{+0.0039}$
c_2	(1000, 10000)	$9605_{-0.0039}^{+0.0039}$
λ	(-1, 1)	$0.0017_{-0.0045}^{+0.0018}$
ω	(-1, 1)	$-0.059_{-0.0027}^{+0.0046}$
H_0	(50, 100)	$69_{-0.004}^{+0.0039}$
χ^2	-	1167.03357

Table 3: The MCMC Results in Pantheon SNe Ia datasets analysis.

The mathematical expression for apparent magnitude $m(z)$ is represented in Eq. (27) and figure 2 shows the contour plots for $c_1, c_2, \lambda, \omega, H_0$ in MCMC analysis of Pantheon SNe Ia datasets. We have applied a wide range priors (10, 1000), (1000, 10000), (-1, 1), (-1, 1), (50, 100) for $c_1, c_2, \lambda, \omega, H_0$, respectively, in our analysis and obtained the best fit values as $c_1 = 244_{-0.0039}^{+0.0039}$, $c_2 = 9605_{-0.0039}^{+0.0039}$, $\lambda = 0.0017_{-0.0045}^{+0.0018}$, $\omega = -0.059_{-0.0027}^{+0.0046}$, $H_0 = 69_{-0.004}^{+0.0039}$ with $1 - \sigma$, $2 - \sigma$ & $3 - \sigma$ errors at 68%, 95% & 99% confidence level, respectively (see Table 3). Our result is compatible with the recent observational datasets.

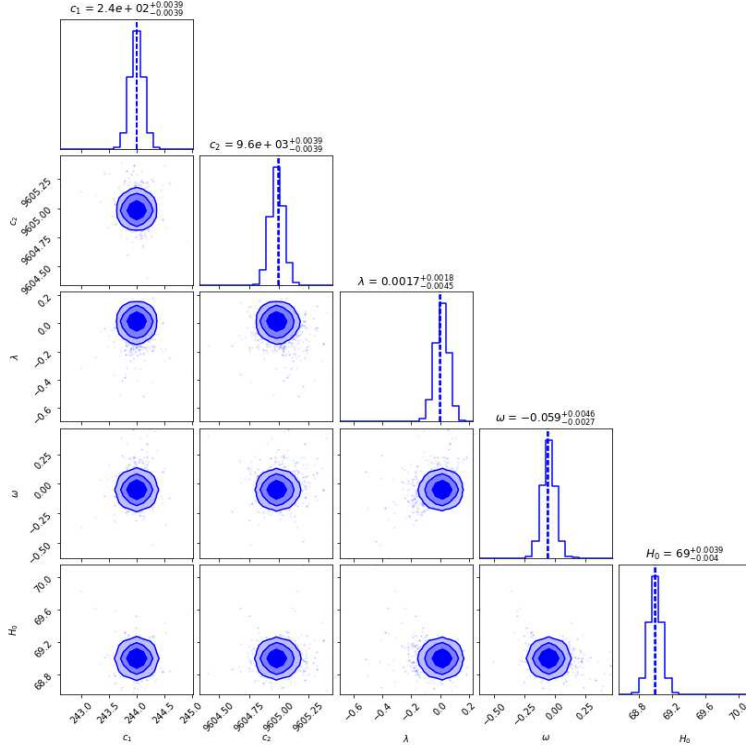


Figure 2: The contour plots of $c_1, c_2, \lambda, \omega, H_0$ in MCMC analysis of the Pantheon SNe Ia samples.

5 Result Analysis and Discussion

In this section, first we introduce matter energy density parameter Ω_m and effective dark energy density parameter Ω_{MG} , respectively as

$$\Omega_m = \frac{\rho}{3(1+\lambda)H^2}, \quad \Omega_{MG} = \frac{c_1}{6(1+\lambda)H}. \quad (28)$$

From Eq. (13), we can define the relationship between energy density parameters Ω_m & Ω_{MG} as

$$\Omega_m + \Omega_{MG} = 1. \quad (29)$$

Equation (28) represents the expressions for matter energy density parameter Ω_m and effective dark energy density parameter Ω_{MG} , respectively. The geometrical evolution of Ω_m, Ω_{MG} , respectively are shown in figure 3a & 3b. Figure 3a depicts that the early universe is matter dominated $\lim_{z \rightarrow \infty} \Omega_m \rightarrow 1$ and in late-time universe $\lim_{z \rightarrow -1} \Omega_m \rightarrow 0$. Figure 3b depicts that late-time universe is dark energy dominated $\lim_{z \rightarrow -1} \Omega_{MG} \rightarrow 1$ and in early time universe $\lim_{z \rightarrow \infty} \Omega_{MG} \rightarrow 0$. At present $z = 0$, we have estimated values of these parameters as $(\Omega_{m0}, \Omega_{MG0}) = (0.37, 0.63), (0.38, 0.62)$, respectively, along two observational datasets $H(z)$ and Pantheon SNe Ia datasets. These values are compatible with recent observations [57]-[62]. The good observations in our model are the effective dark energy term that comes from the geometrical corrections.

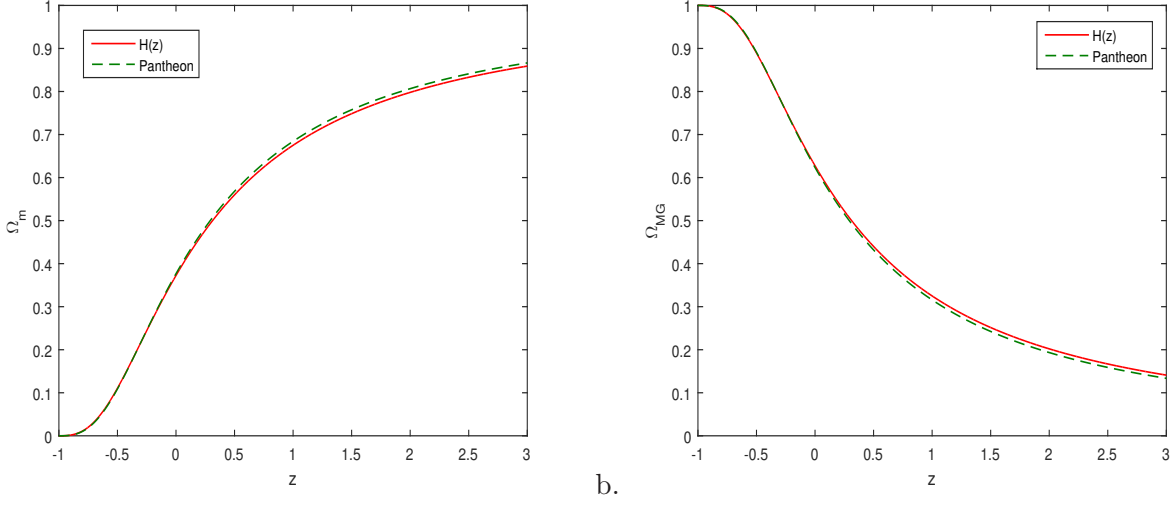


Figure 3: The geometrical evolution of matter energy density parameter Ω_m and effective dark energy density parameter Ω_{MG} over z , respectively.

The effective dark energy equation of state parameter ω_{de} is obtained as

$$\omega_{de} = -1 + \frac{1+z}{3} \frac{H'}{H} - \frac{2\lambda(1+z)H'}{c_1 - 6\lambda H}, \quad (30)$$

or

$$\omega_{de}(z) = -1 + \frac{12(1+\omega)c_2(1+z)^{3(1+\omega)}}{\frac{c_1^2}{1+\lambda} + 24c_2(1+z)^{3(1+\omega)} + c_1\sqrt{\left(\frac{c_1}{1+\lambda}\right)^2 + \frac{24c_2}{1+\lambda}(1+z)^{3(1+\omega)}}} - \frac{6\lambda c_2(1+\omega)(1+z)^{3(1+\omega)}}{\frac{2+c_1\lambda}{2}\sqrt{\left(\frac{c_1}{1+\lambda}\right)^2 + \frac{24c_2}{1+\lambda}(1+z)^{3(1+\omega)}} - \frac{\lambda}{2(1+\lambda)}\left[\left(\frac{c_1}{1+\lambda}\right)^2 + \frac{24c_2}{1+\lambda}(1+z)^{3(1+\omega)}\right]}, \quad \lambda \neq -1. \quad (31)$$

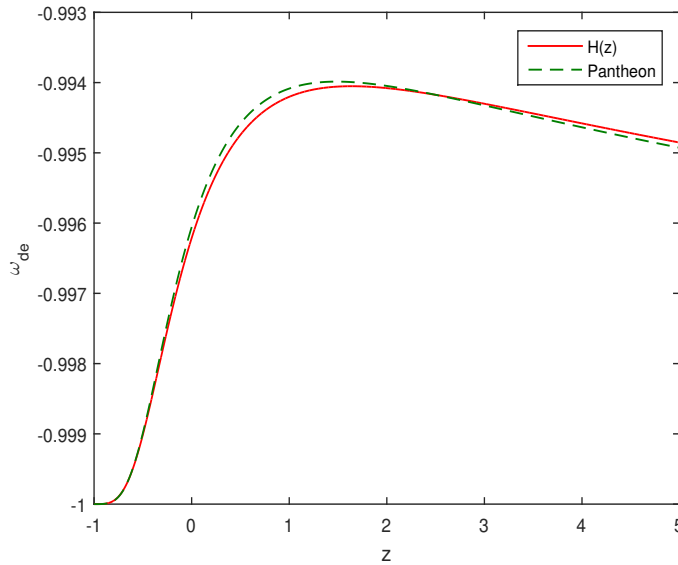


Figure 4: The evolution of effective dark energy equation of state parameter ω_{de} versus z .

The mathematical expression for effective dark energy EoS parameter ω_{de} is represented in Eq. (31) and its geometrical behaviour is shown in figure 4. From figure 4, we can see that effective dark energy EoS varies as $-1 \leq \omega_{de} \leq -0.993$ over the redshift $-1 \leq z \leq 5$. At $z = 0$, we have measured the value of EoS $\omega_{de} = -0.9962, 0.9961$, respectively, along two observational datasets. These values are very closed to the Λ CDM model value.

The expression for deceleration parameter $q(z)$ is represented in Eq. (23) and its geometrical nature is depicted in figure 5. From figure 5, we observe that $\lim_{z \rightarrow -1} q \rightarrow -1$ (accelerating phase of late-time universe) and $\lim_{z \rightarrow \infty} q \rightarrow \frac{1+3\omega}{2} > 0$ (decelerating phase of early universe). At present ($z = 0$) we have estimated the value of deceleration parameter $q_0 = -0.2519, -0.2276$, respectively along two observational datasets $H(z)$ and Pantheon SNe Ia and this reveals that the present phase of the expanding universe is accelerating which is in good agreement with recent observations. From figure 5, one can see that evolution of $q(z)$ shows a signature-flipping (transition) point called as transition redshift z_t at which $q = 0$ i.e., the expansion of universe is in accelerating phase for $z < z_t$ and it is in decelerating expansion phase for $z > z_t$. The general expression for z_t , we have derived from Eq. (23) as below

$$z_t = \left[\frac{c_1^2(2+3\omega)}{6c_2(1+\lambda)(1+3\omega)} \right]^{\frac{1}{3(1+\omega)}} - 1, \quad \lambda \neq -1. \quad (32)$$

In the derived model, we have measured the transition redshift as $z_t = 0.532, 0.435$, respectively, for two observational datasets $H(z)$ and Pantheon SNe Ia. Recently in 2013, Farooq and Ratra [70] have measured this decelerating-accelerating transition redshifts $z_t = 0.74 \pm 0.05$ while Farooq et al. [71] have estimated as $z_t = 0.74 \pm 0.04$. In 2016, Farooq et al. [72] have measured this transition redshifts $z_t = 0.72 \pm 0.05$ and in 2018, Yu et al. [73] have suggested this transition redshifts varies over $0.33 < z_t < 1.0$. Thus, the decelerating-accelerating transition redshift $z_t = 0.532, 0.435$ measured in our model is in good agreement with the results obtained in [70]-[73].

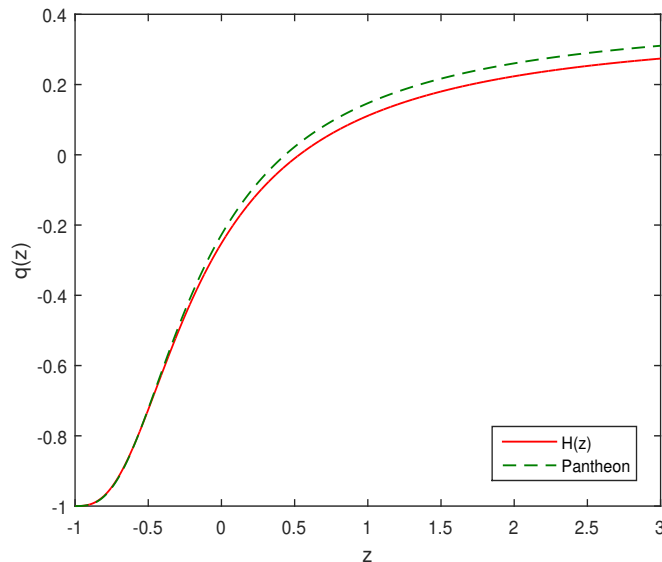


Figure 5: The geometrical evolution of deceleration parameter $q(z)$ versus z .

Om diagnostic analysis

It is simpler to classify concepts related to cosmic dark energy because of the behavior of the Om diagnostic function [74]. For a spatially homogenous universe, the Om diagnostic function is given as

$$Om(z) = \frac{\left(\frac{H(z)}{H_0}\right)^2 - 1}{(1+z)^3 - 1}, \quad (33)$$

where H_0 denotes the current value of the Hubble parameter $H(z)$ as stated in Eq. (22). A negative slope of $Om(z)$ indicates quintessence motion, whereas a positive slope denotes phantom motion. The LambdaCDM model is represented by the constant $Om(z)$.

Using Eq. (22) in (33), we get

$$Om(z) = \frac{\left(\left[\frac{c_1}{12(1+\lambda)} + \frac{1}{12}\sqrt{\left(\frac{c_1}{1+\lambda}\right)^2 + \left(\frac{24c_2}{1+\lambda}\right)(1+z)^{3(1+\omega)}}\right]/H_0\right)^2 - 1}{(1+z)^3 - 1} \quad (34)$$

The mathematical expression for $Om(z)$ function is represented in Eq. (34) and its geometrical behaviour is shown in figure 6. From figure 6, we observe that the slopes are negative along the both datasets $H(z)$ datasets and Pantheon SNe Ia datasets, during evolution of the universe and hence, our model behaves just like quintessence dark energy model. At late-time $\lim_{z \rightarrow -1} Om(z) \rightarrow \left[1 - \frac{c_1^2}{36(1+\lambda)^2 H_0^2}\right]$ which is a constant and it indicates that our model tends to Λ CDM model in late-time scenario.

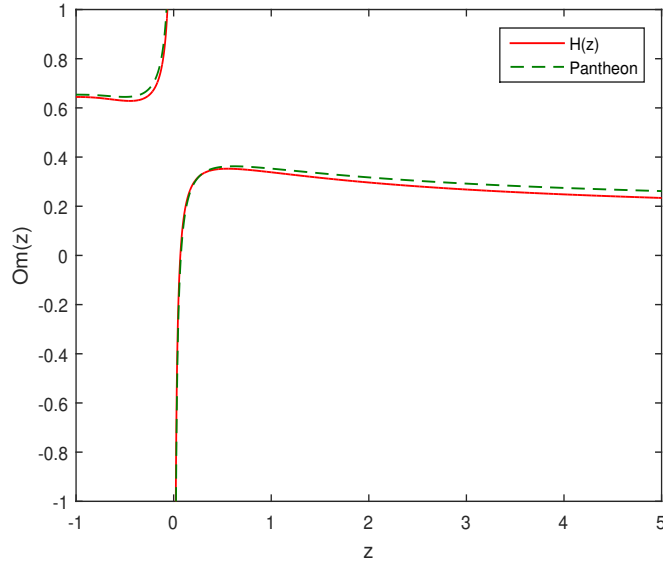


Figure 6: Evolution of $Om(z)$ parameter versus z .

6 Age of the Universe

We define the age of the universe as

$$t_0 - t = \int_0^z \frac{dz}{(1+z)H(z)}, \quad (35)$$

where $H(z)$ is given by Eq. (22). Using this in (35), we have

$$(t_0 - t) = \lim_{z \rightarrow \infty} \int_0^z \frac{dz}{(1+z) \left[\frac{c_1}{12(1+\lambda)} + \frac{1}{12} \sqrt{\left(\frac{c_1}{1+\lambda}\right)^2 + \left(\frac{24c_2}{1+\lambda}\right) (1+z)^{3(1+\omega)}} \right]}. \quad (36)$$

We can see that as $z \rightarrow \infty$, $(t_0 - t)$ tends to a constant value that represents the cosmic age of the universe, $(t_0 - t) \rightarrow t_0 = 0.01423984556, 0.01395722145$, respectively, along two datasets $H(z)$ and Pantheon SNe Ia. The present cosmic age of the universe, we have measured as $t_0 = 13.92, 13.65$ Gyrs, respectively along two observational datasets, which are very closed to observational estimated values. Recently [75, 76] have measured present age of the universe as $t_0 \approx 13.87$ Gyrs.

7 Conclusions

We study various accurate cosmological models in Myrzakulov $F(R, T)$ gravity theory in the current paper. The arbitrary function $F(R, T) = R + \lambda T$ has been investigated, in which R represents the Ricci-scalar curvature, T is the torsion scalar, and λ is an arbitrary constant. After solving the field equations in a flat FLRW spacetime manifold for the Hubble parameter, we estimated the best fit values of the model parameters with $1 - \sigma, 2 - \sigma$, and $3 - \sigma$ regions by utilizing the MCMC analysis. We have conducted a model discussion and outcome analysis using these best fit model parameter conditions. For the best fit shape of Hubble function $H(z)$, we have found the values of model parameters as $c_1 = 247.6^{+0.0048}_{-0.0048}$, $c_2 = 9632^{+0.0048}_{-0.0049}$, $\lambda = 0.0029^{+0.0048}_{-0.0048}$ and $\omega = -0.081^{+0.0048}_{-0.0047}$ at $1 - \sigma, 2 - \sigma$ and $3 - \sigma$ errors for $H(z)$ datasets, and $c_1 = 244^{+0.0039}_{-0.0039}$, $c_2 = 9605^{+0.0039}_{-0.0039}$, $\lambda = 0.0017^{+0.0018}_{-0.0045}$, $\omega = -0.059^{+0.0046}_{-0.0027}$, $H_0 = 69^{+0.0039}_{-0.004}$ with $1 - \sigma, 2 - \sigma$ & $3 - \sigma$ errors at 68%, 95% & 99% confidence level, respectively, for Pantheon SNe Ia datasets (see Table 2 & 3). In the analysis of deceleration parameter $q(z)$, our universe model shows a transit phase dark energy model that is decelerating $q > 0$ for $z > z_t$ and accelerating $q < 0$ for $z < z_t$. We have found the transition redshift $z_t = 0.532, 0.435$, respectively for two observational datasets. We have found the present value of DP as $q_0 = -0.2519, -0.2276$ with Hubble constant $H_0 = 65.5622^{+0.3148}_{-0.3148}, 69^{+0.0039}_{-0.004} \text{ Kms}^{-1} \text{ Mpc}^{-1}$, respectively, for two datasets. The Om diagnostic analysis of $H(z)$ indicates that the current behaviour of our model is quintessential and late-time it approaches to Λ CDM model. We have found that $(\Omega_m, \Omega_{MG}) \rightarrow (0, 1)$ at late-time which is good observations for our model. The effective dark energy equation of state varies as $-1 \leq \omega_{de} \leq -0.993$ with $\omega_{de} \rightarrow -1$ as $z \rightarrow -1$, and the present age of the universe is found as $t_0 = 13.92, 13.65$ Gyrs, respectively for two datasets.

8 Acknowledgments

This work was supported by the Ministry of Science and Higher Education of the Republic of Kazakhstan, Grant AP14870191.

9 Statements and Declarations

Funding and/or Conflicts of interests/Competing interests

The author of this article has no conflict of interests. The author have no competing interests to declare that are relevant to the content of this article. Authors have mentioned clearly all received support from the organization for the submitted work.

References

- [1] S. Capozziello and M. De Laurentis, Extended theories of gravity, *Phys. Rept.* **509**, 167 (2011) [arXiv:1108.6266 [gr-qc]].

- [2] S. Nojiri and S. D. Odintsov, Unified cosmic history in modified gravity: from $F(R)$ theory to Lorentz non-invariant models, *Phys. Rept.* **505**, 59 (2011) [arXiv:1011.0544 [gr-qc]].
- [3] E. J. Copeland, M. Sami and S. Tsujikawa, Dynamics of dark energy, *Int. J. Mod. Phys. D* **15**, 1753 (2006) [hep-th/0603057].
- [4] Y. F. Cai, E. N. Saridakis, M. R. Setare and J. Q. Xia, Quintom cosmology: theoretical implications and observations, *Phys. Rept.* **493**, 1 (2010) [arXiv:0909.2776 [hep-th]].
- [5] N. Bartolo, E. Komatsu, S. Matarrese and A. Riotto, Non-Gaussianity from inflation: Theory and observations, *Phys. Rept.* **402**, 103 (2004) [astro-ph/0406398].
- [6] K. S. Stelle, Renormalization of higher-derivative quantum gravity, *Phys. Rev. D* **16**, 953 (1977).
- [7] T. Biswas, E. Gerwick, T. Koivisto and A. Mazumdar, Towards singularity- and ghost-free theories of gravity, *Phys. Rev. Lett.* **108**, 031101 (2012) [arXiv:1110.5249 [gr-qc]].
- [8] A. De Felice and S. Tsujikawa, $f(R)$ theories, *Living Rev. Rel.* **13**, 3 (2010).
- [9] S. Nojiri and S. D. Odintsov, Modified Gauss-Bonnet theory as gravitational alternative for dark energy, *Phys. Lett. B* **631**, 1 (2005).
- [10] A. De Felice and S. Tsujikawa, Construction of cosmologically viable $f(G)$ gravity models, *Phys. Lett. B* **675**, 1 (2009).
- [11] D. Lovelock, The Einstein tensor and its generalizations, *J. Math. Phys.* **12**, 498 (1971).
- [12] N. Deruelle and L. Farina-Busto, Lovelock gravitational field equations in cosmology, *Phys. Rev. D* **41**, 3696 (1990).
- [13] R. Aldrovandi and J. G. Pereira, Teleparallel Gravity: An Introduction, Springer, Dordrecht (2013).
- [14] J. W. Maluf, The teleparallel equivalent of general relativity, *Annalen Phys.* **525** 339 (2013).
- [15] Y. F. Cai, S. Capozziello, M. De Laurentis and E. N. Saridakis, $f(T)$ teleparallel gravity and cosmology, *Rept. Prog. Phys.* **79** 106901 (2016). [arXiv:1511.07586 [gr-qc]].
- [16] R. Ferraro and F. Fiorini, Modified teleparallel gravity: Inflation without an inflaton, *Phys. Rev. D* **75** 084031 (2007). [gr-qc/0610067].
- [17] E. V. Linder, Einstein's other gravity and the acceleration of the universe, *Phys. Rev. D* **81** 127301 (2010). [arXiv:1005.3039 [astro-ph.CO]].
- [18] G. Kofinas and E. N. Saridakis, Teleparallel equivalent of Gauss-Bonnet gravity and its modifications, *Phys. Rev. D* **90** 084044 (2014). [arXiv:1404.2249 [gr-qc]].
- [19] T. Harko, T. S. Koivisto, F. S. N. Lobo, G. J. Olmo and D. Rubiera-Garcia, Coupling matter in modified Q gravity, *Phys. Rev. D* **98** 084043 (2018). [arXiv:1806.10437 [gr-qc]].
- [20] G. Y. Bogoslovsky and H. F. Goenner, Finslerian spaces possessing local relativistic symmetry, *Gen. Rel. Grav.* **31** 1565 (1999). [gr-qc/9904081].
- [21] N. E. Mavromatos, S. Sarkar and A. Vergou, Stringy space-time foam, Finsler-like metrics and dark matter relics, *Phys. Lett. B* **696**, 300 (2011). [arXiv:1009.2880 [hep-th]].
- [22] A. P. Kouretsis, M. Stathakopoulos and P. C. Stavrinos, Covariant kinematics and gravitational bounce in Finsler space-times, *Phys. Rev. D* **86** 124025 (2012). [arXiv:1208.1673 [gr-qc]].

- [23] S. Basilakos, A. P. Kouretsis, E. N. Saridakis and P. Stavrinos, Resembling dark energy and modified gravity with Finsler-Randers cosmology, *Phys. Rev. D* **88** 123510 (2013). [arXiv:1311.5915 [gr-qc]].
- [24] A. Triantafyllopoulos and P. C. Stavrinos, Weak field equations and generalized FRW cosmology on the tangent Lorentz bundle, *Class. Quant. Grav.* **35** 085011 (2018).
- [25] S. Ikeda, E. N. Saridakis, P. C. Stavrinos and A. Triantafyllopoulos, Cosmology of Lorentz fiber-bundle induced scalar-tensor theories, *Phys. Rev. D* **100** 124035 (2019). [arXiv:1907.10950 [gr-qc]].
- [26] G. Minas, E. N. Saridakis, P. C. Stavrinos and A. Triantafyllopoulos, Bounce cosmology in generalized modified gravities, *Universe* **5** 74 (2019). [arXiv:1902.06558 [gr-qc]].
- [27] F. W. Hehl, J. D. McCrea, E. W. Mielke and Y. Ne'eman, identities, Metric-affine gauge theory of gravity: field equations, Noether identities, world spinors, and breaking of dilation invariance, *Phys. Rept.* **258** 1 (1995). [gr-qc/9402012].
- [28] J. Beltran Jimenez, A. Golovnev, M. Karciauskas and T. S. Koivisto, Bimetric variational principle for general relativity, *Phys. Rev. D* **86** 084024 (2012). [arXiv:1201.4018 [gr-qc]].
- [29] N. Tamanini, Variational approach to gravitational theories with two independent connections, *Phys. Rev. D* **86** 024004 (2012). [arXiv:1205.2511 [gr-qc]].
- [30] R. Myrzakulov, FRW cosmology in $F(R, T)$ gravity, *Eur. Phys. J. C* **72** 2203 (2012). [arXiv:1207.1039 [gr-qc]].
- [31] T. Harko, F. S. N. Lobo, S. Nojiri and S. D. Odintsov, $f(R, T)$ gravity, *Phys. Rev. D* **84** 024020 (2011). [arXiv:1104.2669 [gr-qc]].
- [32] A. Conroy and T. Koivisto, The spectrum of symmetric teleparallel gravity, *Eur. Phys. J. C* **78** 923 (2018). [arXiv:1710.05708 [gr-qc]].
- [33] M. Sharif, S. Rani and R. Myrzakulov, Analysis of $F(R, T)$ gravity models through energy conditions, *Eur. Phys. J. Plus* **128** 123 (2013). [arXiv:1210.2714 [gr-qc]].
- [34] M. Jamil, D. Momeni, M. Raza and R. Myrzakulov, Reconstruction of some cosmological models in $f(R, T)$ cosmology, *Eur. Phys. J. C* **72** 1999 (2012).
- [35] S. Capozziello, M. De Laurentis and R. Myrzakulov, Noether Symmetry Approach for teleparallel-curvature cosmology, *Int. J. Geom. Meth. Mod. Phys.* **12** 1550095 (2015). [arXiv:1412.1471 [gr-qc]].
- [36] P. Feola, X. J. Forteza, S. Capozziello, R. Cianci and S. Vignolo, Mass-radius relation for neutron stars in $f(R) = R + \alpha R^2$ gravity: A comparison between purely metric and torsion formulations, *Phys. Rev. D* **101** 044037 (2020). [arXiv:1909.08847 [astro-ph.HE]].
- [37] Emmanuel N. Saridakis, Shynaray Myrzakul, Kairat Myrzakulov, Koblandy Yerzhanov, Cosmological applications of Myrzakulov gravity, *Phys. Rev. D* **102**, 023525 (2020) [arXiv:1912.03882 [gr-qc]].
- [38] Anagnostopoulos F.K., Basilakos S., Saridakis E.N., Observational constraints on Myrzakulov gravity. [arXiv:2012.06524].
- [39] Myrzakulov N., Myrzakulov R., Ravera L., Metric-Affine Myrzakulov Gravity Theories. [arXiv:2108.00957].
- [40] Iosifidis D., Myrzakulov N, Myrzakulov R., Metric-Affine Version of Myrzakulov $F(R, T, Q, T)$ Gravity and Cosmological Applications. *Universe* 2021, 7, 262. [arXiv:2106.05083]
- [41] Harko T., Myrzakulov N., Myrzakulov R., Shahidi S. Non-minimal geometry-matter couplings in Weyl-Cartan space-times: Myrzakulov $F(R, T, Q, T_m)$ gravity. [arXiv:2110.00358v1].

- [42] R. Saleem, Aqsa Saleem. Variable constraints on some Myrzakulov models to study Baryon asymmetry. *Chinese Journal of Physics*, Volume 84, August 2023, Pages 471-485.
- [43] Iosifidis D., Myrzakulov R., Ravera L., Yergaliyeva G., Yerzhanov K. Metric-Affine Vector - Tensor Correspondence and Implications in $F(R,T,Q,T, D)$ Gravity. [arXiv:2111.14214].
- [44] Papagiannopoulos G., Basilakos S., Saridakis E. N. Dynamical system analysis of Myrzakulov gravity. [arXiv:2202.10871]
- [45] Sobhan Kazempour¹, Amin Rezaei Akbarieh. Cosmological Study in $F(R, T)$ Quasi-dilaton Massive Gravity. [arXiv:2309.09230]
- [46] R. Myrzakulov, Dark energy in $F(R, T)$ gravity, (2021) [arXiv:1205.5266v6 [physics.gen-ph]].
- [47] R. Myrzakulov, Gravity and k -essence, *Gen. Rel. Grav.* **44** 3059–3080 (2012). [arXiv:1008.4486 [astro-ph.CO]].
- [48] D.W. Hogg and D.F. Mackey, Data analysis recipes: Using Markov Chain Monte Carlo, *The Astrophysical Journal Supplement Series* **236** (2018) 18. arXiv:1710.06068 [astro-ph.IM].
- [49] C. Zhang, *et al.*, Four new observational $H(z)$ data from luminous red galaxies in the Sloan Digital Sky Survey data release seven, *Research in Astronomy and Astrophysics*, **14** 1221 (2014).
- [50] J. Simon *et al.*, Constraints on the redshift dependence of the dark energy potential, *Phys. Rev. D* **71** 123001 (2005).
- [51] M. Moresco, *et al.*, Improved constraints on the expansion rate of the Universe up to $z \sim 1.1$ from the spectroscopic evolution of cosmic chronometers, *J. Cosmology Astropart. Phys.*, **8**, 006 (2012).
- [52] M. Moresco, *et al.*, A 6% measurement of the Hubble parameter at $z \sim 0.45$: direct evidence of the epoch of cosmic re-acceleration, *J. Cosmology Astropart. Phys.*, **5**, 014 (2016).
- [53] A. L. Ratsimbazafy, *et al.*, Age-dating luminous red galaxies observed with the Southern African Large Telescope, *MNRAS*, **467**, 3239 (2017).
- [54] D. Stern, *et al.*, Cosmic chronometers: constraining the equation of state of dark energy. I: $H(z)$ measurements, *J. Cosmology Astropart. Phys.*, **2**, 008 (2010).
- [55] N. Borghi, *et al.*, Toward a Better Understanding of Cosmic Chronometers: A New Measurement of $H(z)$ at $z \sim 0.7$, *Astrophys. J. Lett.* **928**, L4 (2022).
- [56] M. Moresco, Raising the bar: new constraints on the Hubble parameter with cosmic chronometers at $z \sim 2$, *MNRAS*, **450**, L16 (2015).
- [57] S. Cao and B. Ratra, $H_0 = 69.8 \pm 1.3 \text{ km s}^{-1} \text{ Mpc}^{-1}$, $\Omega_{m0} = 0.288 \pm 0.017$, and other constraints from lower-redshift, non-CMB, expansion-rate data, *Phys. Rev. D* **107**, 103521 (2023). [arXiv:2302.14203 [astro-ph.CO]].
- [58] S. Cao and B. Ratra, Using lower-redshift, non-CMB, data to constrain the Hubble constant and other cosmological parameters, *MNRAS* **513**, 5686-5700 (2022). [arXiv:2203.10825 [astro-ph.CO]].
- [59] A. Domínguez *et al.*, A new measurement of the Hubble constant and matter content of the Universe using extra-galactic background light γ -ray attenuation, (2019) [arXiv:1903.12097v2 [astro-ph.CO]].
- [60] Chan-Gyung Park, Bharat Ratra, Using SPTpol, Planck 2015, and non-CMB data to constrain tilted spatially-flat and untilted non-flat Λ CDM, XCDM, and ϕ CDM dark energy inflation cosmologies, *Phys. Rev. D* **101**, 083508 (2020). [arXiv:1908.08477 [astro-ph.CO]].

- [61] W. Lin and M. Ishak, A Bayesian interpretation of inconsistency measures in cosmology, *JCAP* **2105**:009, (2021). [arXiv:1909.10991v3 [astro-ph.CO]].
- [62] W. L. Freedman *et al.*, Calibration of the Tip of the Red Giant Branch (TRGB), (2020) [arXiv:2002.01550v1 [astro-ph.GA]].
- [63] S. Birrer *et al.*, TDCOSMO IV: Hierarchical time-delay cosmography – joint inference of the Hubble constant and galaxy density profiles, *A & A* **643**, A165 (2020). [arXiv:2007.02941v3 [astro-ph.CO]].
- [64] Supranta S. Boruah, Michael J. Hudson, Guilhem Lavaux, Peculiar velocities in the local Universe: comparison of different models and the implications for H_0 and dark matter, (2020) [arXiv:2010.01119v1 [astro-ph.CO]].
- [65] Wendy L. Freedman, Measurements of the Hubble Constant: Tensions in Perspective, (2021). arXiv:2106.15656v1 [astro-ph.CO].
- [66] Q. Wu, G. Q. Zhang, F. Y. Wang, An 8% Determination of the Hubble Constant from localized Fast Radio Bursts, (2022) [arXiv:2108.00581v2 [astro-ph.CO]].
- [67] Planck Collaboration, Aghanim N, Akrami Y et al (2020) Planck 2018 results. VI. Cosmological parameters. *A & A* 641:A6. <https://doi.org/10.1051/0004-6361/201833910>. arXiv:1807.06209 [astro-ph.CO]
- [68] Riess AG, Casertano S, Yuan W *et al.* (2021) Cosmic distances calibrated to 1% precision with Gaia EDR3 parallaxes and Hubble Space Telescope photometry of 75 Milky Way Cepheids Confirm Tension with Λ CDM. *ApJ* 908(1):L6. <https://doi.org/10.3847/20418213/abdbaf>. arXiv:2012.08534.
- [69] D. M. Scolnic *et al.*, The complete light-curve sample of spectroscopically confirmed SNe Ia from Pan-STARRS1 and cosmological constraints from the combined pantheon sample, *Astrophys. J.* **859** (2018) 101.
- [70] Omer Farooq, Bharat Ratra, Hubble parameter measurement constraints on the cosmological deceleration-acceleration transition redshift, (2013) [arXiv:1301.5243v1 [astro-ph.CO]].
- [71] Omer Farooq, Sara Crandall, Bharat Ratra, Binned Hubble parameter measurements and the cosmological deceleration-acceleration transition, (2013) [arXiv:1305.1957v1 [astro-ph.CO]].
- [72] Omer Farooq, Foram Madiyar, Sara Crandall, Bharat Ratra, Hubble parameter measurement constraints on the redshift of the deceleration-acceleration transition, dynamical dark energy, and space curvature, (2016) [arXiv:1607.03537v2 [astro-ph.CO]].
- [73] Hai Yu, Bharat Ratra, Fa-Yin Wang, Hubble Parameter and Baryon Acoustic Oscillation Measurement Constraints on the Hubble Constant, the Deviation from the Spatially-Flat Λ cdm Model, The Deceleration-Acceleration Transition Redshift, and Spatial Curvature, (2018) [arXiv:1711.03437v2 [astro-ph.CO]].
- [74] V. Sahni, A. Shafieloo, A. A. Starobinsky, Two new diagnostics of dark energy, *Phys. Rev. D* **78** (2008) 103502.
- [75] A. Pradhan, *et al.*, Modeling Transit Dark Energy in $f(R, L_m)$ -gravity, *Int. J. Geom. Meth. Mod. Phys.* **20** 2350105 (2023).
- [76] D. C. Maurya, Constrained Λ CDM Dark Energy Models in Higher Derivative $F(R, L_m)$ -Gravity Theory, *Phys. Dark Univ.*, **42** (2023) 101373. <https://doi.org/10.1016/j.dark.2023.101373>.